Journal of proteome research

Article

pubs.acs.org/jpr

A Versatile Mass Spectrometry-Based Method to Both Identify Kinase Client-Relationships and Characterize Signaling Network Topology

Nagib Ahsan,[†,‡] Yadong Huang,[†,‡] Alejandro Tovar-Mendez,[†,‡] Kirby N. Swatek,[†,‡] Jingfen Zhang,[‡,§] Ján A. Miernyk,[†,#] Dong Xu,[‡,§] and Jay J. Thelen*[,†,‡]

[†]Department of Biochemistry and Interdisciplinary Plant Group, University of Missouri, Columbia, Missouri 65211, United States

[‡]Christopher S. Bond Life Sciences Center, University of Missouri, Columbia, Missouri 65211, United States

[§]Department of Computer Science and Interdisciplinary Plant Group, University of Missouri, Columbia, Missouri 65211, United States

[#]Plant Genetics Research Unit, USDA, Agricultural Research Service, University of Missouri, Columbia, Missouri 65211, United States

Supporting Information

ABSTRACT: While more than a thousand protein kinases (PK) have been identified in the *Arabidopsis thaliana* genome, relatively little progress has been made toward identifying their individual client proteins. Herein we describe the use of a mass spectrometry-based *in vitro* phosphorylation strategy, termed Kinase Client assay (KiC assay), to study a targeted-aspect of signaling. A synthetic peptide library comprising 377 *in vivo* phosphorylation sequences from developing seed was screened using 71 recombinant *A. thaliana* PK. Among the initial results, we identified 23 proteins as putative clients of 17 PK. In one instance protein phosphatase inhibitor-2 (AtPPI-2) was phosphorylated at multiple-sites by three distinct PK, casein kinase1-like 10, AME3, and a Ser PK-like protein. To confirm this result, full-length recombinant AtPPI-2 was reconstituted with each of these PK. The results confirmed multiple distinct phosphorylation sites within this protein. Biochemical analyses indicate that AtPPI-2 inhibits type 1 protein phosphatase (TOPP) activity, and that the phosphorylated forms of AtPPI-2 are more potent inhibitors. Structural modeling revealed that phosphorylation of AtPPI-2 induces conformational changes that modulate TOPP binding.

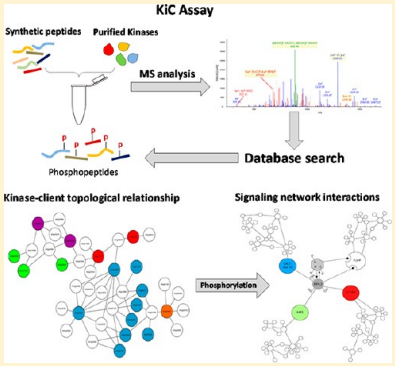

KEYWORDS: *mass spectrometry, kinase, phosphorylation, protein−protein interaction, phosphatase inhibitor, signaling network*

INTRODUCTION

Reversible protein phosphorylation, catalyzed by the coordinated activities of protein kinases (PK) and phosphatases (PP), has been critical to the evolution of complex signaling networks. Both coarse and fine-control of PK and PP activities are essential for regulating the phosphorylation state of a large repertoire of client proteins, which in turn control cellular processes.[1−3] It has been estimated that over 30% of the eukaryotic proteome is phosphorylated, suggesting this is one of the most prevalent types of post-translational regulations.[4] The *Arabidopsis thaliana* genome encodes 1029 PK (both confirmed and predicted), which is proportionally double the number predicted for the human genome.[5] If the specificity of a signal transduction pathway is determined by kinase-mediated phosphorylation of discrete motifs within specific client-proteins, then elucidating the cohort of PK−client relationships is critical to any systematic study.

Advances in mass spectrometry (MS) coupled with the increasing availability of annotated genome sequences have allowed the routine identification of thousands of PK-clients manifested as *in vivo* phosphorylation sites. Integrating these large phosphoproteomic data sets with public sequence databases in repositories such as P[3]DB (http://digbio.missouri.edu/p3db), which includes sequence data from 31 019 phospho-peptides within 10 499 protein sequences derived from five plant species, facilitates comparative analyses of homologous phosphorylation events within related organisms.[6] The *A. thaliana* kinome comprises 1029 PK genes, while a total of 3906 phosphorylation sites have been deposited in P[3]DB indicating a multiplicity of PK-client relationships. Defining these relationships is an essential prelude to understanding the diverse roles in cellular and subcellular signaling, but doing so remains a daunting task[7,8] and is one of the grand challenges facing biologists. To date only a small percentage of these relationships have been defined,[5,7,9] and clearly an improved experimental strategy is warranted.

Identifying PK-clients *in vivo* is a both laborious and challenging endeavor, and is even more so in the absence of background information. *In vitro* approaches can provide preliminary data, which then allows a focus on subsequent validation. A high-throughput method, based on the combination of chemical genetics plus expression of a single epitope-tagged protein, was used to identify yeast PK-clients.[7] Difficulties in applying this strategy to more complex eukaryotes include the availability,

Received: October 23, 2012
Published: December 27, 2012

dx.doi.org/10.1021/pr3009995 | *J. Proteome Res.* 2013, 12, 937−948

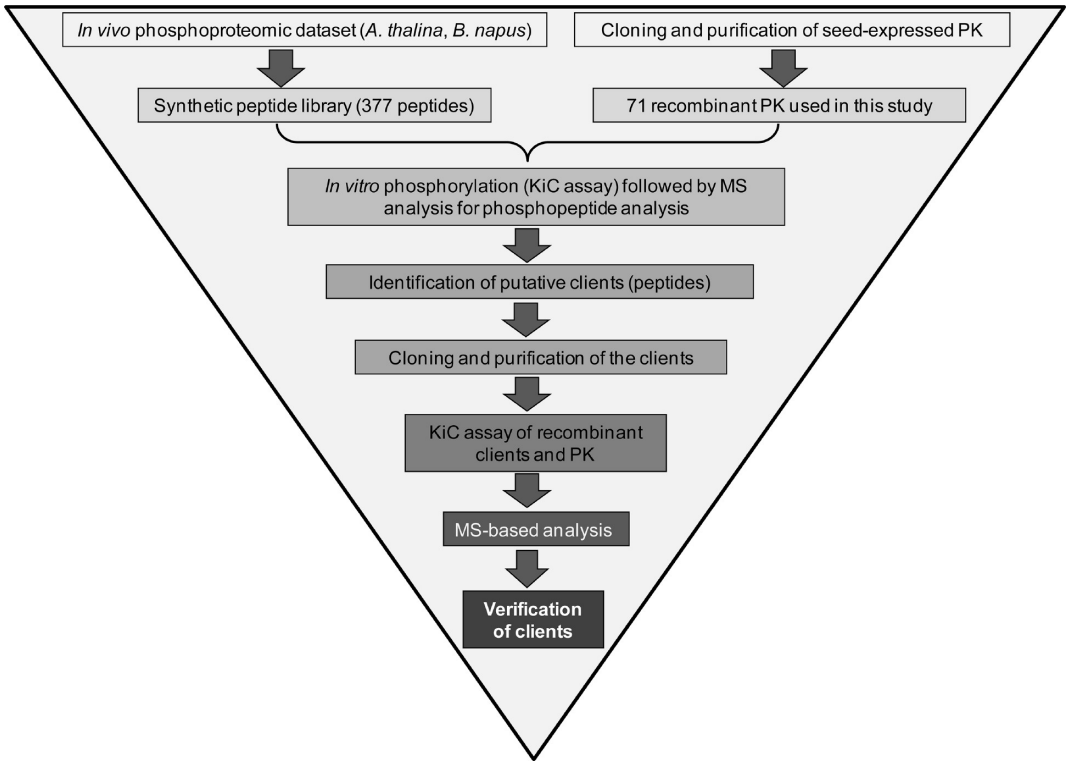

Figure 1. Experimental strategy used for identification of kinase-client relationships.

maintenance, and use of multiple different cell lines. There has been some success using arrayed-protein chips[10] or bead-immobilized PK[11] to identify PK-clients. Feilneret al. used a chip containing 1690 nonredundant proteins to screen potential clients for two *A. thaliana* mitogen-activated protein kinases (MAPK).[12] They identified respectively 48 and 39 potential clients for MPK3 and MPK6. Another strategy, which employs a semidegenerate peptide-array screen coupled with position-specific scoring matrices, followed by *in silico* database querying, has been used to identify potential clients for four *A. thaliana* PK.[5] Alternatively, targeting synthetic peptides derived from analysis of *in vivo* phosphorylation sites, in a chip-based screen, allows a better focus that also serves to validate MS-based phosphorylation site assignments.[13] Each of these methods has utility for identification of PK-clients; however the need for further validation of the interactions with native proteins and for identification of the specific phosphorylation site(s) and phosphorylation preferences at each site remain significant limitations.

Individual proteins can be clients of multiple PK. Therefore any strategy aimed at both identification of PK-client relationships and definition of signaling network topology must include quantitative analysis of phosphorylation-site specificity.[14] Herein we describe the application of a quantitative medium-throughput, label-free, MS-based screen to identify kinase-client relationships in developing *A. thaliana* seeds using a library of 377 synthetic peptides, representing previously identified phosphorylation sites in developing seed of *A. thaliana* and *Brassica napus*. Prior proof-of-concept studies validated use of this screen for analysis of multisite phosphorylation,[15,16] allowing us to also interpret results in terms of phosphorylation-site preference and thus to extend our characterization to include aspects of signaling-network topology.

MATERIALS AND METHODS

Synthetic Peptide Library

On the basis of the results obtained from *in vivo* phosphoproteomic analysis of developing *A. thaliana* and *B. napus* seeds,[17] a library (PEPscreen, Sigma, St. Louis, MO, USA) consisting of 377 synthetic 10−20-mer peptides was designed (Table S1). Stock solutions were prepared by dissolving the peptides in 80% (v/v) dimethylformamide in water to a final concentration of 8 mM. Samples from the stock solutions were then diluted into the KiC assay.[15,16] These synthetic peptides were then used as the basis for an integrated experimental strategy for identification of kinase-client proteins (Figure 1).

Selection of Seed-Expressed PK

Three different criteria were used in selection of the PK to be analyzed. First, expression of PK-encoding genes was monitored using the ATH1 Affymetrix microarray data,[18] from 5, 7, 9, 11, and 13 days after flowering (DAF); those which showed at least 1.1-fold change between the DAF were included. Second, the PK-encoding genes highly expressed during seed development (3−4 DAF, 7−8 DAF, 13−14 DAF, and 18−19 DAF) relative to expression in floral buds, leaves, ovules, roots, seedlings, and stems (http://estdb.biology.ucla.edu/genechip/) were included. Third, the PK-encoding genes expressed during development of *A. thaliana* seeds were identified among the AtGenExpress microarray data available at the PlantsP Web site (http://plantsp.genomics.purdue.edu) and also included.

The *A. thaliana* ecotype Col-0 plants were grown under standard greenhouse long-day (16 h) conditions (22 °C, 50% relative humidity, 144 μmol photons m^{-2} s^{-1}). Total RNA was isolated from young siliques using the RNeasy Mini Kit (Qiagen, Valencia, CA), and cDNAs were synthesized using M-MLV reverse transcriptase (Promega, Madison, WI, USA). The coding regions for each protein were amplified using Pfu

dx.doi.org/10.1021/pr3009995 | J. Proteome Res. 2013, 12, 937−948

polymerase (Stratagene, Santa Clara, CA, USA), plus either PK- (Table S2) or client-specific (Table S3) primers. Purified PCR products were directionally cloned into the Champion pET200 TOPO vector (Invitrogen, Carlsbad, CA, USA) according to the manufacturer's protocol. All constructs were sequenced to verify that no changes had been introduced during amplification.

Recombinant Protein Expression and Purification

For recombinant protein expression, *Escherichia coli* strain BL21 Star (DE3) was transformed by heat-shock. After induction of heterologous protein expression by addition of IPTG to 0.5−1.0 mM, cells were grown with continuous shaking (200 rpm) for 4 h at 37 °C or overnight at 18 °C, depending upon the PK. Cells were harvested by centrifugation at 6000*g* for 15 min. Cell pellets were suspended in 50 mM NaH_2PO_4, pH 8.0, containing 300 mM NaCl, and 10 mM imidazole, then broken by three passages through a French pressure cell at 12 000 psi. Cell debris was removed by centrifugation at 10000*g* for 15 min at 4 °C. Supernatants were loaded onto Ni-NTA affinity columns (Qiagen, Calencia, CA, USA) and, after being washed, bound proteins were eluted with 250 mM imidazole-HCl, pH 8.0, containing 50 mM NaH_2PO_4, and 0.3 M NaCl. Eluted His_6-proteins were dialyzed overnight to remove the imidazole, then stored in 10 mM Tris−HCl, pH 7.5 containing 1 mM DTT and 50% (v/v) glycerol at −20 °C until used. Purity of the PK and client proteins was evaluated by SDS−PAGE using 13% (T) gels.

Protein Kinase Assay

The *in vitro* kinase assay was conducted using recombinant PK (Table S2) plus either a mixture of synthetic peptides or selected full-length client proteins. The KiC assay has been previously described[15,16] and was used with minor modifications (1 h, 37 °C, shaking at 500 rpm). Reactions typically contained a mixture of 100 different peptides, each at a final concentration of 4.5 μM. In the cases of CPKs, reactions additionally contained 0.2 mM $CaCl_2$. The full-length client proteins were assayed at a 2:1 ratio with PK, and reactions were extended to 3 h.

Protein Phosphatase Assay

The phosphoprotein-phosphatase activity of λ PP was estimated by using pNPP as an artificial substrate.[19] Both λ PP (10 μL, 150 ng) and AtPPI-2 (10 μL, 0−700 ng) were diluted in assay buffer containing 50 mM Tris-HCl, pH 7.5, containing 1 mM EDTA, 2 mM $MnCl_2$, 0.5 mg/mL BSA, and 0.1% 2-mercaptoethanol. The λ PP was preincubated with AtPPI-2 at 30 °C for 10 min, followed by addition of pNPP (20 mM,Fluka) in assay buffer followed by incubation for an additional 20 min. Reactions were stopped by adding 150 μL of 0.5 M EDTA, pH 8.0, followed by measuring the A_{405}. All the assays were done at least in triplicate and results are means ± SD for three individual experiments.

Mass Spectrometry

Prior to MS analysis, freeze-dried-peptides were dissolved by adding 40 μL of 0.1% formic acid. Samples were loaded into v-bottom 96-well plates which were then placed onto a pre-chilled 10 °C autosampler. Ten microliters of each sample were analyzed using a Finnigan Surveyor liquid chromatography (LC) system attached to either a stand-alone LTQ-XL or a LTQ Orbitrap XL ETD mass spectrometer (Thermo Fisher, San Jose, CA). During LC, peptides were bound to a C8 Captrap (MichromBioresources, Auburn, CA, USA), eluted with an acetonitrile gradient, and then separated using a "Magic C18" (200 Å, 5 μ bead, Michrom Bioresources, Inc.) fused silica column (10 cm × 150 μm, Polymicro Technologies, Phoenix, AZ). Each column was pre-equilibrated with a gradient of 95% to 5% acetonitrile in 0.1% formic acid prior to MS analysis to clear the C18 matrix of unwanted ions.

Analysis of the synthetic peptide screen was performed using a stand-alone LTQ-XL. Instrument settings were described previously[15,20] except the gradient was increased to 1−40% acetonitrile. Analysis of the recombinant protein kinase client assays was performed using a LTQ Orbitrap XL ETD. Full-length proteins were digested with sequencing grade trypsin (Promega, Madison, WI). Tryptic peptides were fragmented using either collision induced dissociation (CID) or "decision tree" methods, which utilizes both CID and ETD during a single sample analysis.[21] Nanospray ionization source parameter settings were ion spray voltage (kV), 2.10; capillary temperature (°C), 250; capillary voltage (v), 36; and tube lens (v), 90. Precursor masses were scanned with the analyzer set to FTMS; mass range, normal; resolution, 60000 or 100000; scan type, positive mode; data type, centroid; and a scan range of 200−2000 m/z. The 10 most abundant ions from the precursor scan were selected for subsequent fragmentation using the ion trap-analyzer, normal mass range, normal scan rate, and centroid data type. Charge-state screening and monoisotopic precursor-selection modes were enabled. Unassigned charge states and masses with a charge state of +1 were not analyzed. The CID data-dependent scan settings included: collision energy 35 kV, default charge state +2, isolation width 2.0 m/z, activation time of 30 ms (msec), and multistage activation was disabled. Dynamic exclusion was enabled with a repeat count of 3, repeat duration of 30 ms, exclusion list size 50−100, and exclusion duration of 30 ms. Data-dependent ions fragmented with ETD had an exclusion mass width of 10 ppm. Decision tree settings were previously described[21] (Swaneyet al., 2008). The reagent ion source settings including temperature, emission current, energy level, and CI pressure were 160 °C, 50 μA, −70 V, and 17.5 psi, respectively. The activation time was 100 ms and supplemental activation mode was enabled.

Bioinformatic Analysis

The raw MS files were searched against a decoy database consisting of the random complement of the sequences comprising the peptide library, using SEQUEST algorithms (Proteome Discoverer 1.0, Thermo Fisher). Instrument and search parameters settings have been previously described.[15,20] For recombinant kinase-client assays, a composite target decoy database was constructed based upon all full-length kinases and client protein sequences. The search parameters were mass type, average precursor plus fragment; dynamic modifications, phosphorylation of Ser/Thr/Tyr (+79.9799 Da) and oxidation of Met (+15.9994 Da), and the static modification, of Cys-carboxyamidomethylation. Additional parameters included two missed tryptic cleavage sites; an absolute threshold of 1000; a minimum ion count of 10; mass range, 200−2000, and a precursor and fragment ion tolerance of 1000 ppm and 1 Da, respectively.

Identification data were evaluated using the XCorr function of SEQUEST, and phosphorylation-site localization was accomplished using phospho*RS* (Proteome Discoverer, v. 1.0.3, Thermo Fisher). The XCorr values for each charge state were set to default, and no decoy hits were allowed. Peptide mass deviation was 10 ppm and a setting of two peptides/protein was used to further filter the data. For final validation, each spectrum was

dx.doi.org/10.1021/pr3009995 | *J. Proteome Res.* 2013, 12, 937−948

inspected manually and accepted only when the phosphopeptide had the highest pRS site probability, pRS score, XCorr value and site-determining fragment ions allowed unambiguous localization of the phosphorylation site. Phosphopeptides with a pRS score ≥50 and/or a pRS site probability of ≥55% were accepted.

Modeling of Native and Mutant AtPPI-2

For the target protein AtPPI-2 (At5g52200), MUFOLD was used to predict the local structure and the solvent accessibility of the target, then used to scan PDB to obtain the target/template alignments. The best templates are 2O8G_I, 2O8A_I and 2O8A_J. The best target/template alignments cover almost 84% target residues; however only 26% of the aligned residues from the templates have structure information. Thus, MUFOLD was used to search and evaluate fragmentary structures which fit the target in the terms of sequence, local structure, and similarity of solvent accessibility, and which also fit the templates in terms of structure. Fragments from 1Z5U_A, 1YA9_A, and 2DFS_A were selected. The structural constraints from both templates and fragments were used with MUFOLD to build the target model, then applied in a multilayer evaluation approach including molecular dynamics ranking and consensus quality assessment to select the near-native predicted model.[22,23] For analysis of the modified sequences, the Ser residue at position 140 was changed to the P-Ser-mimics Glu or Asp.

RESULTS

Identification of Client Proteins for Seed-Expressed Kinases

Among the 377 synthetic peptides used as clients for 71 seed specific recombinant PK, a total of 23 peptides were phosphorylated by 17 PK (Table 1); several PK phosphorylated more than one peptide (Table S4). The 17 PK that were active in our *in vitro* assay include two members of the casein kinase family (At3g23340 and At5g67380), one receptor-like cytoplasmic kinase (At3g55450), two LAMMER-family kinases (At4g24740 and At4g32660), and 12 CPK or CPK-like (At5g04870, At4g23650, At2g17290, At5g19450, At1g35670, At2g31500, At5g66210, At3g19100, At5g24430, At2g17530, At4g35500, and At5g22840) kinases (Table 1). The 23 peptides that were phosphorylated in the KiC assay are derived from a wide range of proteins including a protein phosphatase inhibitor (A5g52200), cytochrome P450 (At3g30290), aquaporin (At2g37180), chaperonin (At4g25580), and transcription factor (At4G38900) (Table 1). All of these proteins have previously been reported to be phosphorylated *in vivo* (P^3DB).

Peptides GDFDADsDDEIVLVPK (At4g17060), GIADYSASPDVKsER (At3g16310), and ITGNFPAsKLSQDLQR (At5g61140) were phosphorylated at a single site and by a single recombinant PK, while peptides TSLHStRtVPLVPW (At1g02410), IGEIENRstFLLAVK (At3g25690), and KTPNLGGPsMKsMSGGNL (At3g16760) were phosphorylated at two sites by a single PK (Table 1). A total of nine client peptides were phosphorylated either at a single or multisites by two different PK. In most of the cases, the same family PK shared common clients and phosphorylated at the same residues. For instance, peptide KPKIAIAsVFGNDSDED correspond to D111/G-patch protein (At5g26610) is phosphorylated at the same Ser residues by both the CK1-like 10 (At3g23340) and CK1A (At5g67380) (Table 1). Our results indicate that clients of the same family PK's overlap extensively (Table 1). There were also instances where a single peptide was a client of multiple groups of PK's. The best example of this is peptide IHDDDDDEGsLsPRGGR corresponding to AtPPI-2 (At5g52200), which was phosphorylated by CK1-like 10, AME3, and a Ser-PK-like protein (Table 1).

Validation of the Peptide-Based KiC Assay Results

It is important that the results obtained with synthetic peptides be validated using full-length proteins as clients. We have begun to address this point by focusing on AtPPI-2, which is a putative client for three PK (Table 1). After heterologous expression, the full-length recombinant protein was purified (Figure S1), and the KiC assay was repeated with the recombinant kinases and AtPPI-2 followed by MS analysis (Figure 1). While agreement among the *in vivo* phospho-proteomic data set, the *in vitro* peptide results, and the *in vitro* full-length recombinant client protein results was not perfect, ultimately it was all-encompassing. Most of the synthetic peptides were multisite phosphorylated. The most extreme example has three phosphorylation sites (Table S4). Multisite phosphorylation is not, however, unusual in terms of cellular signaling. In some instances of multistep signaling networks, a "primed phosphorylation mechanism" is necessary where "residue X" must be phosphorylated as a prelude to subsequent phosphorylation of "residue A", which is the functional site of regulation/signaling.[24]

In most cases, the phosphorylation sites observed *in vitro* were the same as those identified *in vivo* (Table S4). There were, however, a few exceptions involving synthetic peptides based upon the *B. napus* phospho-proteomic results where a phosphorylation site that had been identified *in vivo* could not be detected during MS analysis of the native protein. For instance, recombinant AME3 was able to phosphorylate Ser residues in the *B. napus*-based synthetic peptide IHDDDDDEGsLsPRGGR corresponding to PPI-2 protein but not the single Ser residue in the related *A. thaliana* peptide TPYHPMMDDDGSLSPR using purified recombinant protein. Results from examination of the MS data prior to filtering seemed to indicate the presence of P-Ser; however the results were not of sufficient quality based upon FDR assessment. Overall, the results seen in this study support the large majority of phosphorylation sites of many proteins observed previously *in vivo*. In addition, many novel phosphorylation sites were identified within the AtPPI-2 sequence (Table S5).

Kinase-Specific Phosphorylation Preferences in AtPPI-2, a Type-One Protein Phosphatase Inhibitor

Our results clearly show that a single client can be targeted by multiple PK. As a model, we have focused on AtPPI-2 as a client. AtPPI-2 is a type-one protein phosphatase inhibitor that inhibits the activities of all nine type-one phosphatases from *A. thaliana*.[19] A total of 14 phosphorylation sites were reported in AtPPI-2 by several *in vivo* phosphoproteomic studies (P^3DB); however the PK responsible for these phosphorylation events remain unknown. Employing the KiC assay with purified, recombinant AtPPI-2 we found a total of five *in vivo* sites phosphorylated by three different PK (Figure 2A). Comparison of these results with those available in public phosphorylation databases P^3DB and PhosPhAt additionally revealed that phosphorylation of Ser^{77} and Thr^{178} had not previously been reported (Figure 2A). For example, MS/MS spectrum of the phosphopeptide NVLNDAAASsSR which showed many b and y product ions (including the phosphorylated Ser) and the phosphate neutral loss on either fragment or precursor ions (Figure 2B) provides clear evidence of phosphorylation of Ser^{77}. A relative comparison of phosphorylated to nonphosphorylaed

dx.doi.org/10.1021/pr3009995 | J. Proteome Res. 2013, 12, 937−948

Table 1. *Arabidopsis* Seed Expressed Putative Kinase Clients Identified by KiC Assay[a]

	protein kinases																
Putative clients	CK1-like 10 (At3g23340)	CK1A (At5g67380)	RLC-PK (At3g55450)	AME1 (At4g24740)	AME3 (At4g32660)	PKc-L (At2g17530)	SRPK1 (At4g35500)	Ser PK like (At5g22840)	CRK2 (At3g19100)	CRK4 (At5g24430)	CPK1 (At5g04870)	CPK3 (At4g23650)	CPK6 (At2g17290)	CPK8 (At5g19450)	CPK11 (At1g35670)	CPK24 (At2g31500)	CPK28 (At5g66210)
PPI-2 (At5g52200)	×				×			×									
D111/G-patch protein (At5g26610)	×	×															
FRIGIDA interact 2 (At4g17060)	×																
MPPN family (At3g16310)	×																
Myb protein 1 (At1g76970)	×		×														
RNA helicase (At5g61140)			×														
Calthrin light chain (At3g51890)			×						×	×				×			×
Cytochrome c CtaG (At1g02410)			×														
CHUP1 protein (At3g25690)			×														
Cytochrome P450 (At3g30290)			×														
RSZp22 splicing factor (At2g24590)				×	×	×		×									
DUF1296 (At3g13990)				×		×	×										
FPA protein (At2g43410)				×	×												
CAP160 protein (At4g25580)				×	×												
Aquaporin PIP2−3 (At2g37180)										×	×	×		×	×	×	×
Chaperonin CPN60 (At3g13860)											×	×	×		×		×
DUF3511 (At3g13910)												×			×		
GYF domain-contain protein (At1g24300)												×			×		
Protein uncharacterized (At3g50370)												×			×		×
bZIP_1 transcription factor (At4g38900)												×		×	×		
PPR containing protein (At5g43830)												×			×	×	
Transmembrane proteins 14C (At1g33265)														×	×		
TPR containing protein (At3g16760)															×		

[a]A total of 23 peptides were phosphorylated by 17 recombinant kinases.

dx.doi.org/10.1021/pr3009995 | J. Proteome Res. 2013, 12, 937−948

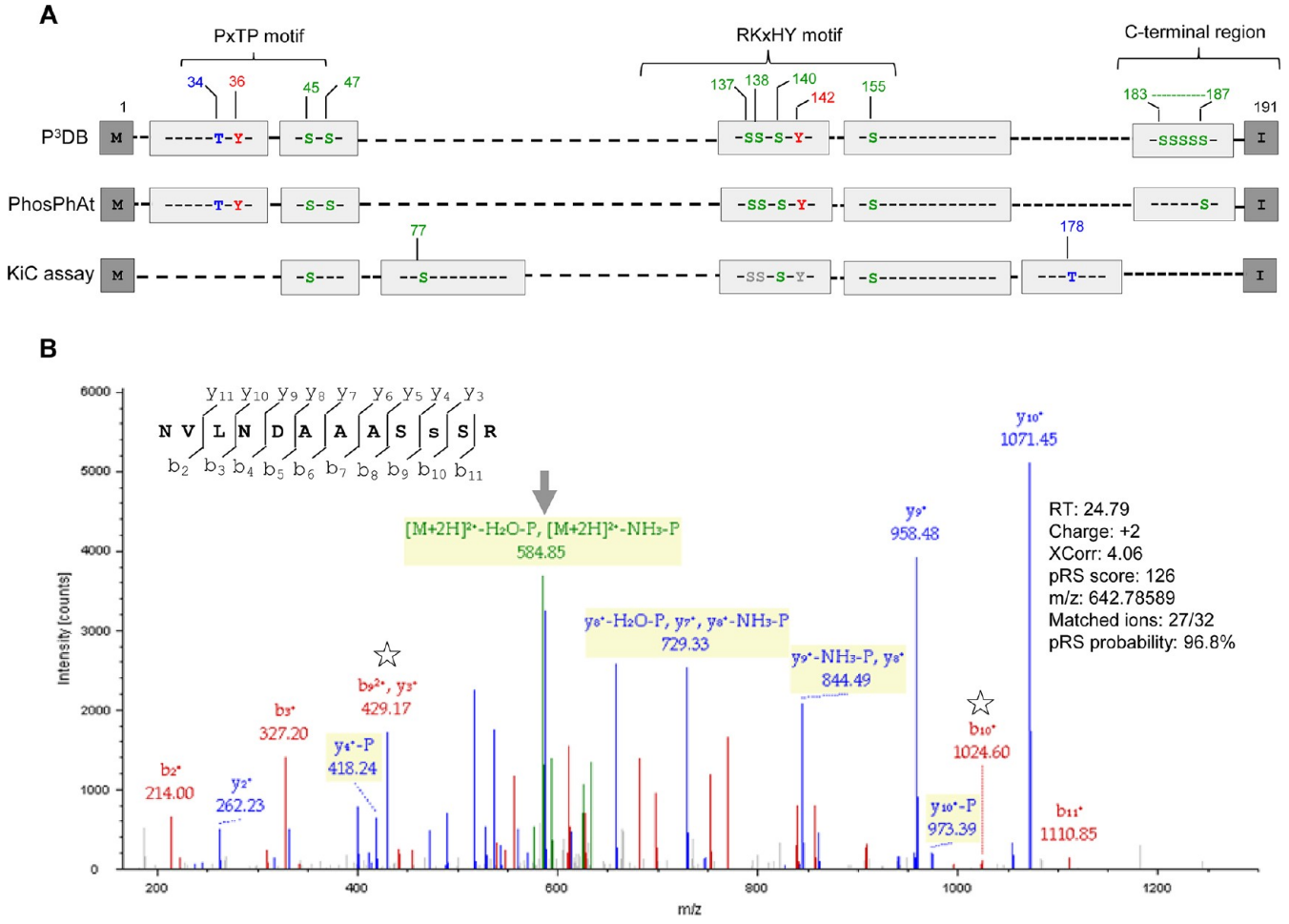

Figure 2. Comparative phosphosites mapping of AtPPI-2 (At5g52200). Experimentally determined, *in vivo* phosphorylation sites for AtPPI-2 from P^{3}DB and PhosPhAt database, compared with sites obtained *in vitro* (KiC assay) using recombinant AtPPI-2 and PK (CK1 like-10, AME3 and Ser PK like protein) (A). Letters in gray indicates low-confidence phosphosites. (B) An MS/MS spectrum of a novel phosphosite in AtPPI-2. The phosphopeptide NVLNDAAASsSR represents an example of an additional novel phosphosite (Ser^{77}) of the AtPPI-2. Small letter in the sequence indicating the phosphosite. Arrow and asterisks indicate the detection of the neutral loss of the phosphate on fragments or precursor ions and the phosphorylated Ser residues, respectively.

sites for AtPPI-2 showed that phosphorylation status varies with specific sites and kinase (Figure S2). Notably, Ser^{155} was only phosphorylated by AME3, whereas Ser^{45} was phosphorylated by CK1-like 10 and Ser-PK-like protein (Figure 3).

While there are individual PK-specific sites (e.g., Ser^{45} and Ser^{77}) present in the AtPPI-2 sequence, a C-terminal region characterized by a RKxHY motif includes a Ser^{140} site that was phosphorylated by all three kinases. Full-sequence phosphorylation site preferences were quantified by spectral counting. The results indicate that Ser^{45} was the site most extensively phosphorylated; however, this site was not phosphorylated by all three kinases, whereas the Ser^{140} site was the second most phosphorylated site, and additionally was phosphorylated by all three PK (Figure 3). Although in the RKxHY motif, Ser$^{137, 138}$ and Tyr^{142} were also phosphorylated by all three kinases, due to low (>50) pRS score and pRS site probability these sites were considered as low confidence (Figure 3). It is important to note, however, that *in vivo* phosphorylation of Ser$^{137, 138, 140}$ and Tyr^{142} has been previously reported (P^{3}DB).

Inhibition of Type 1 Protein Phosphatase (TOPP) Activity byAtPPI-2

To evaluate the effect(s) of AtPPI-2 phosphorylation on TOPP-inhibiting activity, we used the distantly related lambda phosphatase (λ PPase) as a surrogate since the sequence and structural features responsible for TOPP docking of PPI-2 inhibitor are conserved[25] (Figure S3). To determine the inhibitory effect of AtPPI-2, pNPP was used as substrate for λ PPase. Initial results using nonphosphorylated recombinant AtPPI-2 showed a dose-dependent inhibition of λ PPase with an IC_{50} near 140 ng (Figure S4A). Inhibition was time-dependent, reaching 80% by 30 min (Figure S4B). Recombinant AtPPI-2 was also phosphorylated by a single kinase, combinations of two PK, or all three PK prior to assaying PPase inhibition. Inhibitory activity was expressed as a percentage of the control value (λ PPase activity without AtPPI-2). The results showed phosphorylated AtPPI-2 was a more potent inhibitor of λ PPase than nonphosphorylated protein (Figure 4). Among the various combinations, there were substantial differences in inhibition efficacy. The most potent form of the inhibitor was that phosphorylated by CK1-like 10 and either of the remaining PK (Figure 4). Overall, the results show that phosphorylated AtPPI-2 is a more potent *in vitro* inhibitor of TOPP activity and imply the potential for effective multisite phosphorylation as a component of a signaling network.

dx.doi.org/10.1021/pr3009995 | J. Proteome Res. 2013, 12, 937−948

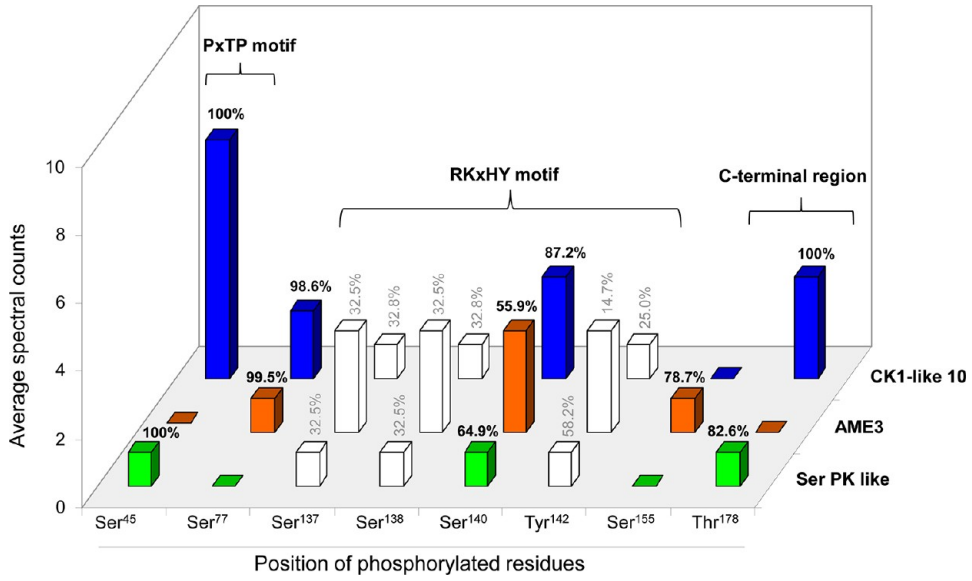

Figure 3. Comparison of the *in vitro* phosphorylation-site specificities of recombinant CK1-like 10, AME3, and Ser PK like protein. In separate experiments, recombinant AtPPI-2 was phosphorylated with an individual kinase, digested with trypsin, and the tryptic peptides analyzed by MS. Data presented are means of three biological replicates. Percentage shown above the bars indicates the pRS site probability for each amino acid. On the basis of the pRS score and pRS site probability (Table S5) solid and empty bars represent the phosphosites with high and low confidence, respectively.

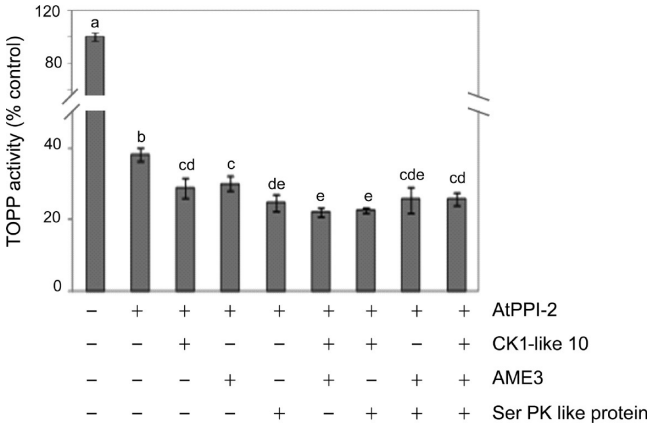

Figure 4. Phosphorylation of AtPPI-2 makes it a better inhibitor of λ TOPP activity. Recombinant AtPPI-2 was incubated with λ TOPP either before or after phosphorylation by the indicated kinases. TOPP activity was measured at an absorbance A_{405} wherein *p*-nitrophenyl phosphate (pNPP) was used as substrate. Inhibitory activity is expressed as a percentage of the control values. Values are means ± SEM for control ($n = 9$) or plus AtPPI-2 ($n = 3$) reactions. Different letters above the bars indicate a statistically significant difference ($p < 0.05$) according to the Duncan multiple-range test.

DISCUSSION

A relatively small number of experimental strategies have been applied to PK-client identification.[5,9,11−13,26] Although useful, none of these methods offer the resolution necessary for characterization of either multisite or multi-PK phosphorylation, both requisite for dissecting complex signaling networks. In the present study, we present results obtained using a previously described medium-throughput analysis, the "KiC assay",[15,16] which measures *in vitro* phosphorylation of synthetic peptides. The library of peptides described herein is based on the sequences of 377 *in vivo* phosphorylation sites and was screened with 71 recombinant PK. Almost all of the 71 PK were active based upon auto phosphorylation analyses (data not shown), and thus indiscriminate phosphorylation of the 377 peptides was a possible outcome. However, this was not observed. Only 17 PK showed activity against this equimolar peptide library, phosphorylating a grand total of 23 peptides (Table 1). In most instances, the *in vitro* results (Table S4) recapitulate the results obtained from *in vivo* phosphorylation-site analysis.[17]

Because many proteins integrate signals from multiple PK, quantitative analyses of individual sites are required to develop a better understanding of how signaling networks function.[13,14] We have identified several proteins as potential clients for multiple PK. The topological relationships among *A. thaliana* seed-expressed PK and their cognate client-proteins were determined (Figure 5). As expected, the preferred clients for the CPK family members exhibited a range of specificity and redundancy that ultimately reflects kinase similarity. The client connectivity among unrelated kinases was surprising and may offer clues about the potential for cross-talk between signal transduction pathways. One of the peptides that was phosphorylated by multiple kinases belonged to the TOPP regulatory protein PPI-2 (At5g52200), a potential hub in an as-yet undiscovered signaling network (Figure 5).

The AtPPI-2 primary sequence is 58−81% similar to other plant orthologs, and the phosphorylation sites themselves are conserved (Figure S5). Comparison of the phosphorylation sites of *A. thaliana* and mammalian PPI-2 (human or mouse) revealed comparatively fewer sites in the plant protein (16 versus 19 and 11, respectively) than human (Figure S6A). Phosphorylation at the N-terminal PxTPY motif of PPI-2 is conserved in both plants and animals; however, phosphorylation at the PP-binding RKxHY motif has thus far been identified only in plant PPI-2 (Figure S6B). It has been previously established that mammalian PPI-2 is phosphorylated by multiple PK, and that phosphorylation is important for both selectivity and activity as an inhibitor.[27,28] We observed that the situation is similar in the plant-derived system but with additional elaborations. The Thr-residue within the PxT^{72}P motif is

dx.doi.org/10.1021/pr3009995 | J. Proteome Res. 2013, 12, 937−948

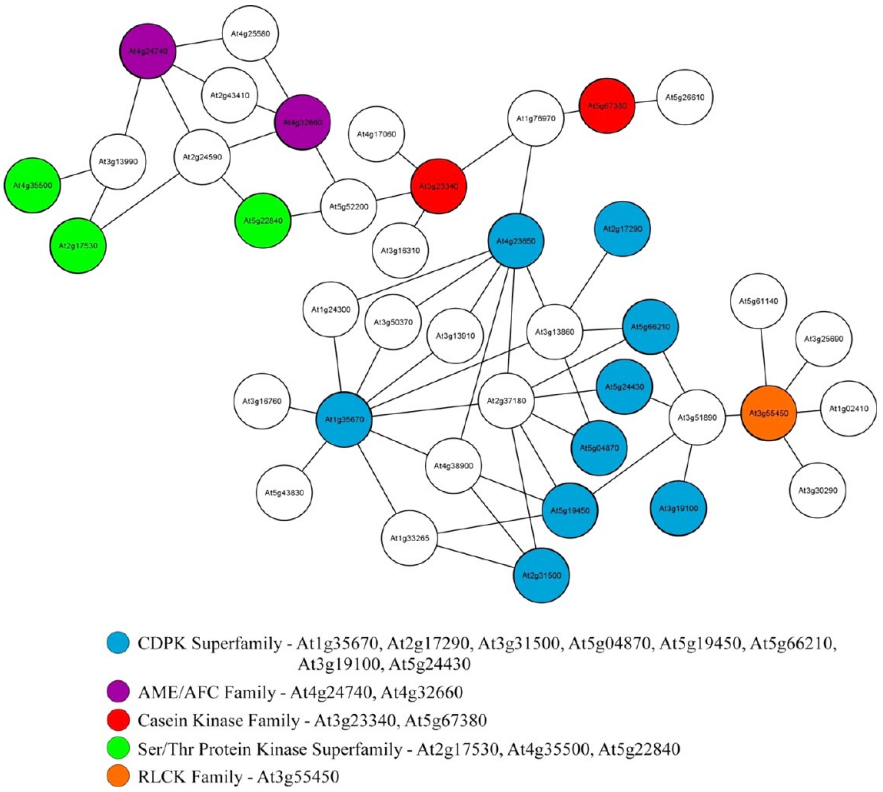

Figure 5. The topological relationships among *A. thaliana* seed-expressed PK and their cognate client-proteins. The data were obtained by *in vitro* screening of a synthetic peptide library derived from *in vivo* phospho-proteomic analyses of developing *A. thaliana* and *B. napus* seeds (P^3DB) with 71 recombinant *A. thaliana* PK. Upon the basis of the peptide sequences, 23 proteins were identified as presumptive clients for 17 PK. The cartograph was assembled using the organic layout from Cytoscape version 2.3.2.[38] The PKs that belong to the same family are presented as hubs of the same color, while the client nodes are uncolored. Each edge represents a single PK-client pair. The spatial distribution of hubs, nodes, and edges is arbitrary.

phosphorylated in mammalian cells by glycogen shaggy-like protein kinase-3 (GSK3) and cyclin-dependent protein kinases 2 (CDC2).[28−30] The *A. thaliana* homologues of these two PK were included in our study (Table S2); however, they did not phosphorylate the "Thr^{72}"-containing peptide (Table S4). In contrast, we observed that AtPPI-2 was phosphorylated at multiple sites by the CK1-like 10, AME3, and Ser PK-like PK (Figure 2). There is no report that homologues of these plant PK phosphorylate mammalian PPI-2, although a CK2 family protein does phosphorylate a Ser residues near the PxTPY motif of human PPI-2.[31]

Results from analyses of phosphorylation-site preferences indicate that Ser^{45} was the most intensely phosphorylated site of any individual PK, whereas the Ser^{140} residue was strongly phosphorylated by three different PK (Figure 3). Additional support for the importance of multisite phosphorylation comes from crystallography and 3-D modeling analyses of mouse PPI-2 which revealed that residues 130−169 near the C-terminal RKxHY motif are directly involved in both protein interactions and inhibition of TOPP catalytic (c) activity.[31] This region is highly conserved among plants (Figure S5) and between *A. thaliana* and mouse PPI-2 (Figure S6). Moreover, comparative 3-D modeling of this conserved region supports a similar interaction between the nonphosphorylated form of AtPPI-2 with Arg^{96}, His^{125}, Arg^{221}, and Tyr^{272} of TOPPc (Figure 6) to that previously demonstrated with the mouse proteins.[31] To determine whether phosphorylation in the RKxHY motif could alter the interaction of TOPPc-PPI-2 binding structure, Ser^{140} which is phosphorylated by all three kinases was mimicked by either Glu or Asp (Figure 6C,D). Interestingly, the 3-D modeling showed that phosphorylation of Ser^{140} in this region produces conformational changes (Figure 6) that could affect binding.[32,33]

Participation of AtPPI-2 in a regulatory signaling network could be amplified by phosphorylation-dependent modulation of TOPP activity. To evaluate this possibility we employed a reconstitution assay consisting of recombinant AtPPI-2 and λ-PP. We observed that the phosphorylated forms of AtPPI-2 had significantly higher PP-inhibitory activity in comparison with the nonphosphorylated form (Figure 4), and this activity is affected by location and degree of phosphorylation. Consistent with our model, it has been reported that phosphorylation of human PPI-1 at Thr^{35} and Ser^{67}produces a potent inhibitor of TOPP activity, whereas no inhibitory effect was observed in the nonphosphorylated form.[34]

More recently it has been observed that human PPI-2 forms an inactive complex with TOPP that can be reversed by phosphorylation of Thr^{72} by GSK3 or CDC2 kinases.[35] Currently the precise role of phosphorylation of different amino acids at AtPPI-2 in inhibition of TOPP remains largely unverified; however 3-D modeling and crystallography studies of mammalian PPI-2[36] provide support for the proposal that phosphorylation of amino acids in the TOPP binding motif may play a role in a conformational change that affects the binding and/or inhibition activity (Figure 5). Moreover it has been suggested that the action of one kinase enhances phosphorylation of other residues by different kinases and is required for potentiation of different kinase action.[30] Although the RVxF, PxTPY, and RKxHY motifs are conserved among *Arabidopsis* and mammalian PPI-2,

dx.doi.org/10.1021/pr3009995 | *J. Proteome Res.* 2013, 12, 937−948

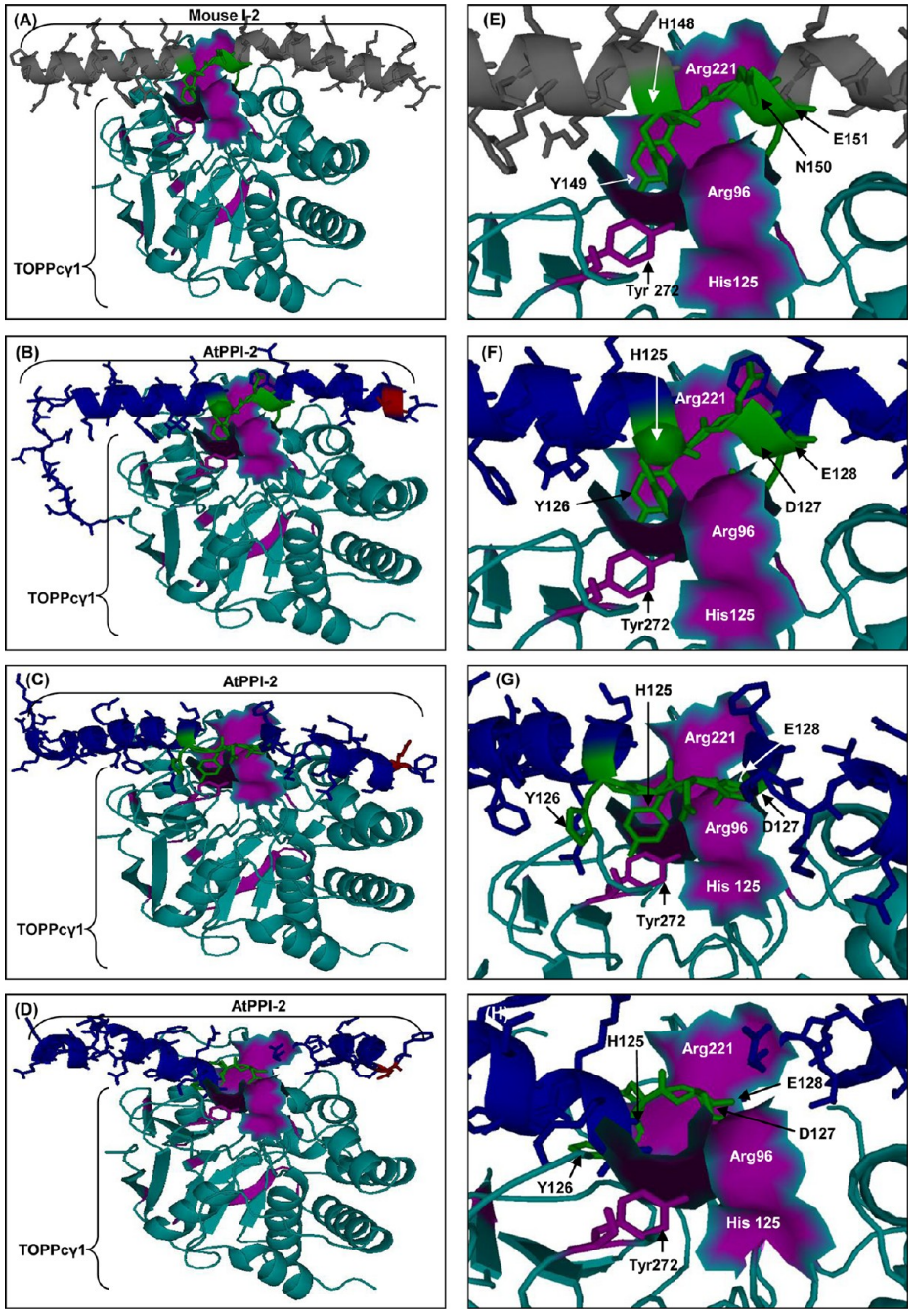

Figure 6. Predicted conformational changes in the AtPPI-2 structure induced by phosphorylation of Ser^{140}. Panel (A) includes the model of the rat TOPP catalytic domain γ1 subunit (cyan, PDB accession 2O8AA0) docked with mouse PPI-2 (purple, PDB accession 2O8AI0). Panels B, C, and D contain the model of the rat TOPP catalytic domain docked with nonphosphorylated (B) or phosphorylated (C and D) AtPPI-2, respectively. Protein phosphorylation was mimicked by Ser to Glu (C) and Asp (D) changes. Phosphorylation of Ser^{140} cause conformational changes in AtPPI-2. Panels E, F, G and H include close-up views of the interaction between the conserved RKxHYmotif of mouse PPI-2 (E) and/or AtPPI-2 (F, G) with residues Arg^{96}, His^{125}, Arg^{221}, and Tyr^{272} of TOPP. The AtPPI-2 binding sites in TOPP are colored magenta. Structures were produced using PyMOL (www.pymol.org).

some features of the mammalian PPI-2 such as the SGILK and SQ motifs at the N-terminal region are believed to be responsible for the TOPP interaction,[31] but these motifs are absent in AtPPI-2 (Figure S6). Therefore, it could be possible that phosphorylation events act differently between the *Arabidopsis* and mammalian PPI-2. Upon the basis of our results and those of others, we propose a working model that includes the involvement of AtPPI-2 in complex network-signaling interactions (Figure 7). This model shows AtPPI-2 is located at the interface of multiple signaling networks. It has been reported that the inactive form (unphophorylated) of AtPPI-2 could inhibit all nine TOPP in *Arabidopsis*.[19] The phosphorylated form of AtPPI-2 is, however, a more effective protein-phosphatase inhibitor wherein activation can be mediated through phosphorylation of AtPPI-2 by three separate kinases (CK 1-like 10, AME3, or a Ser/Thr PK-family protein), any pair of these kinases, or all three kinases. Conceptually, phosphorylation of APPI-2 would result from transduction of a signal from the respective kinase network.

dx.doi.org/10.1021/pr3009995 | *J. Proteome Res.* 2013, 12, 937−948

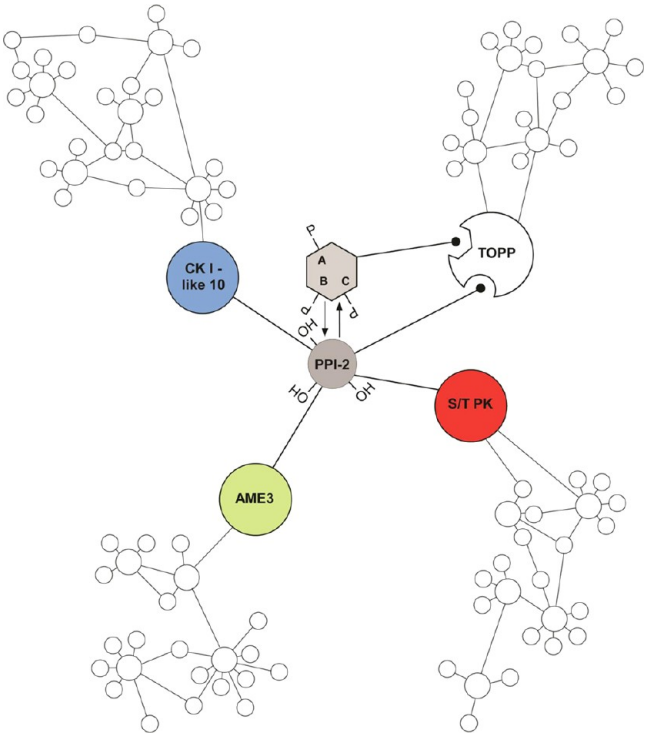

Figure 7. Analysis of the topology of signaling network interactions. This model shows AtPPI-2 located at the interface of multiple signaling networks. Both inactive and activated (phosphorylated) forms of AtPPI-2 bind to TOPP, inhibiting protein-phosphatase activity. The phosphorylated form of AtPPI-2 is, however, a more effective protein-phosphatase inhibitor. In this model, activation of AtPPI-2 can be mediated through phosphorylation by three separate kinases (CK 1-like 10, a LAMMER-type protein kinase (AME3), or a Ser/Thr PK-family protein), any pair of these kinases, or all three kinases. In all instances, phosphorylation of PPI-2 would result from transduction of a signal from the affiliated network. A, B, and C represent phosphorylated residues. In the nonphosphorylaed form they are represented by -OH groups, while in the activated form of AtPPI-2 they are designated by -P. A (CK 1-like 10) includes Ser^{45}, Ser^{77}, Ser^{140}, and Thr^{178}; B (AME3), Ser^{77}, Ser^{140}, and Ser^{155}; and C (S/T PK-like), Ser^{45}, Ser^{140}, and Thr^{178}. This model depicts the complexity of interactions (multiple networks, kinases, and phosphorylation-sites) that might be controlled from a single-interface among pathways.

We have previously established the utility of the KiC assay for analysis of defined PK/client pairs, as well as for PK-client discovery.[15,16,20] Although in this experiment, we limited ourselves to synthetic peptides corresponding to known *in vivo* phosphorylation sites of the proteins of *Arabidopsis* and *B. napus* developing seeds, a library including all of the potential Ser, Thr, and Tyr-containing tryptic peptides and maximum number of recombinant PK could scale up to encompass the majority of the potential clients for each PK. However, this would be impractical in terms of expense. And even if this were not the case, it would still be constrained by issues such as the necessity of prior phosphorylation (or some other post-translational modification) of site 1 before site 2 can be phosphorylated, the potential of a hierarchy of phosphorylation, phosphorylation-mediated protein interactions, etc.

In principle, the use of multiple PK with an individual synthetic peptide would allow the quantitative phosphorylation preferences of each PK to be determined. Furthermore, we demonstrate this extension to the PK-client identification strategy and reveal an additional application of the assay for the identification/characterization of the topology of signaling networks (Figure 5). Our results suggest that AtPPI-2 occupies a position at the intersection of multiple signaling pathways. Stangeret al.[37] recently reported a similar topological position for the yeast adaptor protein, Nbp2p, which influences protein phosphatase function. It is thus possible that inhibitor or adapter proteins could occupy important positions as global regulators for specific protein phosphatases or classes of protein phosphatases, as reported here.

■ ASSOCIATED CONTENT

Supporting Information

Table S1. Synthetic peptide library used for KiC assay.

Table S2. List of the forward and reverse primers of seed expressed protein kinases.

Table S3. List of the forward and reverse primers of putative kinase clients.

Table S4. Putative kinase clients identified by KiC assay.

Table S5. Mass spectrometric-based phosphorylation analysis of recombinant AtPPI-2 with their corresponding kinases.

Figure S1. Expression and purification of recombinant client protein (At5g52200, protein phosphatase inhibitor-2) and its corresponding kinases. The PCR product was cloned into pET-200 vector and the construct was transformed into BL21 (DE3) competent cells, and cultures were induced with IPTG and lyses were collected after 4 h. The IPTG induced (+) or not induced (−) lysate, flow-through (after-Ni), washes (W1−2) and eluted fractions (E1-E3) were separated by SDS-PAGE (13%) and stained with CBB. Right panel represents the purified kinases, At3g23340, casein kinase I-like 10; At4g32660, LAMMER-type protein kinase (AME3); and At5g22840, Ser/Thr protein kinase family protein.

Figure S2. Relative phosphorylation abundance of AtPPI-2. In separate experiments, recombinant AtPPI-2 was phosphorylated with an individual kinase, digested with trypsin, and the tryptic peptides analyzed by MS. The histogram depicts the spectral counts of the both phosphopeptide and nonphosphorylaed. The data presented are means of three biological replicates.

Figure S3. Amino acid sequence alignment of *Arabidopsis* type 1 protein phosphatase (TOPP) isoforms with bacterial lambda and human PP1γ. Residues identified as important for the interaction and bind with inhibitor-2 are shown by arrows.

Figure S4. Inhibition of λPPase activity by AtPPI-2. TOPP activity was measured at an absorbance A_{405} wherein *p*-nitrophenyl phosphate (pNPP) was used as substrate. TOPP activity was expressed as percentage of the values of λ PP1 and pNPP at a 30 min reaction time without inhibitor protein (PPI-2). (A) Effect of AtPPI-2 in phosphatase activity; (B) effect of reaction time in TOPP activity. Error bars represent the mean ± SE (n = 9 for control and n = 3 for other reactions).

Figure S5. Amino acid sequence alignment of *Arabidopsis* protein phosphatase inhibitor-2 (AtPPI-2) with other plants homologues. Shaded boxes indicating the phosphosites identified in P^3DB and in this study. Type one protein phosphatase binding/interacting motifs are marked.

Figure S5. Comparison of the amino acid sequence of AtPPI-2 with mammalian (human and mouse) PPI-2. (A) Schematic representation of the plant and mammalian PPI-2 with their identified phosphosites. Phosphorylation sites at AtPPI-2 were identified either in the current study or in the

dx.doi.org/10.1021/pr3009995 | J. Proteome Res. 2013, 12, 937−948

phosphoproteomic data sets in P^{3}DB and the current experiment. Mammalian phosphoproteome database http://www.phosphosite.org and http://phospho.elm.eu.org were used to identify the phosphosites of human and mouse PPI-2. (B) The amino acid sequence alignment of AtPPI-2 with mammalian (human and mouse) PPI-2. Shaded boxes indicating the phosphorylated residues identified experimentally (*in vivo* and/or *in vitro*). Motifs important for TOPP binding or inhibition are marked.[19] This material is available free of charge via the Internet at http://pubs.acs.org.

AUTHOR INFORMATION

Corresponding Author

*Address: Department of Biochemistry, 271G Christopher S. Bond Life Sciences Center, 1201 Rollins Ave, University of Missouri, Columbia, MO 65211, USA. Telephone: 573 884-1325. Fax: 573 884-9676. E-mail: thelenj@missouri.edu.

Notes

The authors declare no competing financial interest.

ACKNOWLEDGMENTS

The contribution of ML Johnston to the networking graphics presented is gratefully acknowledged. Research in the Thelen Lab is supported by the NSF (Grant No. DBI-0604439).

REFERENCES

(1) Kim, T. W.; Guan, S.; Sun, Y.; Deng, Z.; Tang, W.; Shang, J. X.; Sun, Y.; Burlingame, A. L.; Wang, Z. Y. Brassinosteroid signal transduction from cell-surface receptor kinases to nuclear transcription factors. *Nat. Cell Biol.* **2009**, *11*, 1254−1260.

(2) Breitkreutz, A.; Choi, H.; Sharom, J. R.; Boucher, L.; Neduva, V.; Larsen, B.; Lin, Z.-Y.; Breitkreutz, B.-J.; Stark, C.; Liu, G.; Ahn, J.; Dewar-Darch, D.; Reguly, T.; Tang, X.; Almeida, R.; Qin, Z. S.; Pawson, T.; Gingras, A.-C.; Nesvizhskii, A. I.; Tyers, M. A global protein kinase and phosphatase interaction network in yeast. *Science* **2010**, *328*, 1043−1046.

(3) Tang, W.; Yuan, M.; Wang, R.; Yang, Y.; Wang, C.; Oses-Prieto, J. A.; Kim, T. W.; Zhou, H. W.; Deng, Z.; Gampala, S. S.; Gendron, J. M.; Jonassen, E. M.; Lillo, C.; DeLong, A.; Burlingame, A. L.; Sun, Y.; Wang, Z. Y. PP2A activates brassinosteroid-responsive gene expression and plant growth by dephosphorylating BZR1. *Nat. Cell Biol.* **2011**, *13*, 124−131.

(4) Cohen, P. T. W. Protein phosphatase 1: Targeted in many directions. *J. Cell Sci.* **2002**, *115*, 241−256.

(5) Vlad, F.; Turk, B. E.; Peynot, P.; Leung, J.; Merlot, S. A versatile strategy to define the phosphorylation preferences of plant protein kinases and screen for putative substrates. *Plant J.* **2008**, *55*, 104−117.

(6) Gao, J.; Agrawal, G. K.; Thelen, J. J.; Xu, D. P^{3}DB: a plant protein phosphorylation database. *Nucleic Acids Res.* **2009**, *37*, D960−D962.

(7) Dephoure, N.; Howson, R. W.; Blethrow, J. D.; Shokat, K. M.; O'Shea, E. K. Combining chemical genetics and proteomics to identify protein kinase substrates. *Proc. Natl Acad. Sci. U. S. A.* **2008**, No. 105, 10762−10767.

(8) Lee, T. Y.; Bretaña, N. A.; Lu, C. T. PlantPhos: using maximal dependence decomposition to identify plant phosphorylation sites with substrate site specificity. *BMC Bioinf.* **2011**, No. 12, 261.

(9) Curran, A.; Chang, I. F.; Chang, C. L.; Garg, S.; Miguel, R. M.; Barron, Y. D.; Li, Y.; Romanowsky, S.; Cushman, J. C.; Gribskov, M.; Harmon, A. C.; Harper, J. F. Calcium-dependent protein kinases from *Arabidopsis* show substrate specificity differences in an analysis of 103 substrates. *Front. Plant Sci.* **2011**, *2*, 36.

(10) Lee, D. W.; Kim, H. J.; Choi, C. H.; Shin, J. H.; Kim, E. K. Development of a protein chip to measure PKCβ activity. *Appl. Biochem. Biotechnol.* **2011**, *163*, 803−812.

(11) Zhang, M.; Han, G.; Wang, C.; Cheng, K.; Li, R.; Liu, H.; Wei, X.; Ye, M.; Zou, H. A bead-based approach for large-scale identification of *in vitro* kinase substrates. *Proteomics* **2011**, *11*, 4632−4637.

(12) Feilner, T.; Hultschig, C.; Lee, J.; Meyer, S.; Immink, R. G.; Koenig, A.; Possling, A.; Seitz, H.; Beveridge, A.; Scheel, D.; Cahill, D. J.; Lehrach, H.; Kreutzberger, J.; Kersten, B. High throughput identification of potential *Arabidopsis* mitogen-activated protein kinases substrates. *Mol. Cell Proteomics* **2005**, *4*, 1558−1568.

(13) de la Fuente van Bentem, S.; Anrather, D.; Dohnal, I.; Roitinger, E.; Csaszar, E.; Joore, J.; Buijnink, J.; Carreri, A.; Forzani, C.; Lorkovic, Z. J.; Verhounig, A.; Jonak, C.; Hirt, H. Site-specific phosphorylation profiling of *Arabidopsis* proteins by mass spectrometry and peptide chip analysis. *J. Proteome Res.* **2008**, *7*, 2458−2470.

(14) Olsen, J. V.; Blagoev, B.; Gnad, F.; Macek, B.; Kumar, C.; Mortensen, P.; Mann, M. Global, *in vivo*, and site-specific phosphorylation dynamics in signaling networks. *Cell* **2006**, *127*, 635−648.

(15) Huang, Y.; Houston, N. L.; Tovar-Mendez, A.; Stevenson, S. E.; Miernyk, J. A.; Randall, D. D.; Thelen, J. J. A quantitative mass spectrometry-based approach for identifying protein kinase clients and quantifying kinase activity. *Anal. Biochem.* **2010**, *402*, 69−76.

(16) Huang, Y.; Thelen, J. J. KiC assay: a quantitative mass spectrometry-based approach for kinase client screening and activity analysis. *Methods Mol. Biol.* **2012**, *893*, 359−370.

(17) Meyer, L. J.; Gao, J.; Xu, D.; Thelen, J. J. Phosphoproteomic analysis of seed maturation in *Arabidopsis*, rapeseed, and soybean. *Plant Physiol.* **2012**, *159*, 517−528.

(18) Chen, M.; Mooney, B. P.; Hajduch, M.; Joshi, T.; Zhou, M.; Xu, D.; Thelen, J. J. System analysis of an *Arabidopsis* mutant altered in de novo fatty acid synthesis reveals diverse changes in seed composition and metabolism. *Plant Physiol.* **2009**, *150*, 27−41.

(19) Templeton, G. W.; Nimick, M.; Morrice, N.; Campbel, D.; Goudreault, l. M.; Gingras, A. C.; Takemiya, A.; Shimazaki, K.; Moorhead, G. B. Identification and characterization of AtI-2, an *Arabidopsis* homologue of an ancient protein phosphatase 1 (PP1) regulatory subunit. *Biochem. J.* **2011**, *435*, 73−83.

(20) Ahsan, N.; Swatek, K. N.; Zhang, J.; Miernyk, J. A.; Xu, D.; Thelen, J. J. Scanning mutagenesis of the amino acid sequences flanking phosphorylation site 1 of the mitochondrial pyruvate dehydrogenase complex. *Front. Plant Sci.* **2012**, *3*, 153.

(21) Swaney, D. L.; McAlister, G. C.; Coon, J. J. Decision tree-driven tandem mass spectrometry for shotgun proteomics. *Nat. Methods* **2008**, *5*, 959−964.

(22) Zhang, J.; Wang, Q.; Barz, B.; He, Z.; Kosztin, I.; Shang, Y.; Xu, D. (2009) MUFOLD: A new solution for protein 3D structure prediction. *Proteins* **2009**, *78*, 1137−1152.

(23) Zhang, J.; Wang, Q.; Vantasin, K.; Zhang, J.; He, Z.; Kosztin, I.; Shang, Y.; Xu, D. A multi-layer evaluation approach for protein structure prediction and model quality assessment. *Proteins* **2011**, *79*, S10: 172−184.

(24) terHaar, E.; Coll, J. T.; Austen, D. A.; Hsiao, H. M.; Swenson, L.; Jain, J. Structure of GSK3 beta reveals a primed phosphorylation mechanism. *Nat. Struct. Biol.* **2001**, *8*, 593−596.

(25) Zhou, S.; Clemens, J. C.; Hakes, J. D.; Bradford, D.; Dixon, J. E. Expression, purification crystallization and biochemical characterization of a recombinant protein phosphatase. *J. Biol. Chem.* **1993**, *268*, 17754−17761.

(26) Pusch, S.; Harashima, H.; Schnittger, A. Identification of kinase substrates by bimolecular complementation assays. *Plant J.* **2012**, *70*, 348−356.

(27) Leach, C.; Shenolikar, S.; Brautigan, D. L. Phosphorylation of phosphatase inhibitor-2 at centrosomes during mitosis. *J. Biol. Chem.* **2003**, *278*, 26015−26020.

(28) Li, M.; Stefansson, B.; Wang, W.; Schaefer, E. M.; Brautigan, D. L. Phosphorylation of the Pro-X-Thr-Pro site in phosphatase inhibitor-2 by cyclin-dependent protein kinase during M-phase of the cell cycle. *Cell Signal.* **2006**, *18*, 1318−1326.

(29) Wang, Q. M.; Guan, K. L.; Roach, P. J.; DePaoli-Roach, A. A. Phosphorylation and activation of the ATP-Mg-dependent protein phosphatase by the mitogen-activated protein kinase. *J. Biol. Chem.* **1995**, *270*, 18352−18358.
(30) Park, I. K.; Roach, P.; Bondor, J.; Fox, S. P.; DePaoli-Roach, A. A. Molecular mechanism of the synergistic phosphorylation of phosphatase inhibitor-2. Cloning, expression, and site-directed mutagenesis of inhibitor-2. *J. Biol. Chem.* **1994**, *269*, 944−954.
(31) Hurley, T. D.; Yang, J.; Zhang, L.; Goodwin, K. D.; Zou, Q.; Cortese, M.; Dunker, A. K.; DePaoli-Roach, A. A. Structural basis for regulation of protein phosphatase 1 by inhibitor-2. *J. Biol. Chem.* **2007**, *282*, 28874−28883.
(32) Ohki, S.; Eto, M.; Kariya, E.; Hayano, T.; Hayashi, Y.; Yazawa, M.; Brautigan, D.; Kainosho, M. (2001) Solution NMR structure of the myosin phosphatase inhibitor protein CPI-17 shows phosphorylation-induced conformational changes responsible for activation. *J. Mol. Biol.* **2001**, *314*, 839−849.
(33) Zhang, H.; Shen, W.; Rempel, D.; Monsey, J.; Vidavsky, I.; Gross, M. L.; Bose, R. Carboxyl-group footprinting maps the dimerization interface and phosphorylation-induced conformational changes of a membrane-associated tyrosine kinase. *Mol. Cell. Proteomics***2011**, 10, M110.005678.
(34) Huang, K. X.; Paudel, H. K. Ser67-phosphorylated inhibitor 1 is a potent protein phosphatase 1 inhibitor. *Proc. Natl Acad. Sci. USA* **2000**, *97*, 5824−5829.
(35) Dancheck, B.; Ragusa, M. J.; Allaire, M.; Nairn, A. C.; Page, R.; Peti, W. (2011) Molecular investigations of the structure and function of the protein phosphatase 1-spinophilin-inhibitor 2 heterotrimeric complex. *Biochemistry* **2011**, *50*, 1238−1246.
(36) Eto, M.; Kitazawa, T.; Matsuzawa, F.; Aikawa, S.; Kirkbride, J. A.; Isozumi, N.; Nishimura, Y.; Brautigan, D. L.; Ohki, S. Y. (2007) Phosphorylation-induced conformational switching of CPI-17 produces a potent myosin phosphatase inhibitor. *Structure* **2007**, *15*, 1591−1602.
(37) Stanger, K.; Gorelik, M.; Davidson, A. R. Yeast adaptor protein, Nbp2p, is conserved regulator of fungal Ptc1p phosphatases and is involved in multiple signaling pathways. *J. Biol. Chem.* **2012**, *287*, 22133−22141.
(38) Shannon, P.; Markiel, A.; Ozier, O.; Baliga, N. S.; Wang, J. T.; Ramage, D.; Amin, N.; Schwikowski, B.; Ideker, T. Cytoscape: a software environment for integrated models of bimolecular interaction networks. *Genome Res.* **2003**, *13*, 2498−2504.